

Modeling the Impact of Recurrent Collaterals In CA3 on Downstream CA1 Firing Frequency

Teryn Johnson Gladys Ornelas Srihita Rudraraju
t8johnso@eng.ucsd.edu glornela@eng.ucsd.edu srrudrar@eng.ucsd.edu

Department of Bioengineering
University of California,
San Diego La Jolla, CA 92093

Abstract

The Hippocampal regions CA3 and CA1 have been demonstrated to play a role in memory consolidation and spatial navigation. Recurrent Collaterals (RC) in CA3 Pyramidal cells serve as a feedback mechanism onto CA3 cells while Schaffer Collaterals (SC) directly project synaptic inputs from CA3 to CA1. The neuronal activity from RC and SC have been associated with Long-term Potentiation, gamma frequencies, and Sharp-Wave Ripples oscillations (SWR), activities present during events believed to be related to long-term memory storage. This project explored the effects of altering the number of synaptic connections within each region and between the two regions. By varying the probability that synaptic connections will form in CA3's RC and the SC, it was determined that there was a non-obvious and non-linear effect for each region's ability to be engaged in a particular firing frequency. It was found that approximately a ten percent connection between both the Schaffer collaterals and the recurrent collaterals best engaged CA3 and CA1 in gamma and ripple frequencies.

1 Introduction

The Hippocampus, a region of the brain located underneath the cerebral cortex, is a well-studied structure widely considered the main structure responsible for memory formation and consolidation (Fig.1). In recent years, much of the research within the hippocampus has been dedicated towards understanding place cells. Place cells are cells hypothesized to encode spatial information about a subject's environment and is useful for navigation and spatial awareness [11]. Some recent work, however, has been dedicated towards understanding how stimulation of regions local to the hippocampus can best facilitate neuronal engagement [12]. In particular, this study has shown that varying frequency of stimulation causes nonlinear neuronal engagement [12]. This work has been a large step forward in understanding how information is transferred within the hippocampus. As a next step, this project explores a way of estimating the number of connections that best facilitates a particular frequency band. The hippocampus has been shown to primarily engage in theta, gamma, and ripple frequency ranges [1] [4]. By determining the number of connections that best engages the hippocampus with these particular frequencies, a general estimate can be made in how many synaptic connections are formed between regions of the hippocampus.

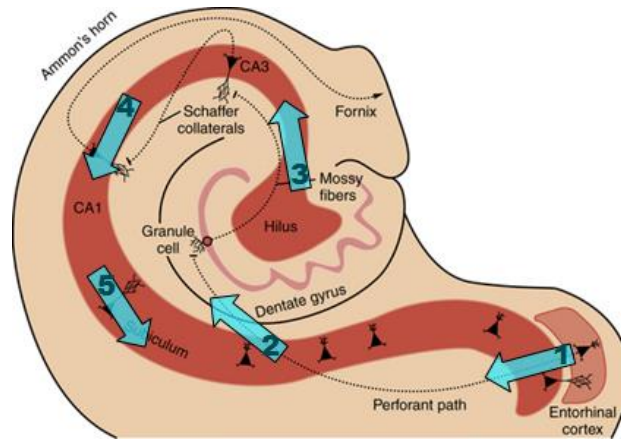


Figure 1: Hippocampal Formation as reprinted from *Neurophysiology of Seizure and Epilepsy* (2015) [14] and memory consolidation pathway. (1) The event synapse travels through the Perforant Pathway originating from the Entorhinal Cortex into the (2) Dentate Gyrus (DG). From the DG the signal projects through the (3) Mossy Fibers into region CA3. Schaffer Collaterals from CA3 stimulate (4) Pyramidal Cells in CA1. The synapse travels through the (5) Subiculum where it will then be stored in the Neocortex (not shown) for long term storage.

The Hippocampus is separated into four regions, CA1, CA2, CA3, and CA4. For the purpose of memory consolidation, research has demonstrated a correlation between neuronal activity in regions CA3 and CA1 during events related to long-term memory formation [15]. Communication between CA3 and CA1 occurs directly through SC [13]. Meanwhile CA3 receives feedback inhibition through its RC [8]. The synaptic firing frequency of RC and SC are believed to induce long-term potentiation (LTP) as well as the gamma and theta frequencies that occur during memory formation [10]. The memory formation involves the activation of a pattern of neurons in the hippocampus. The synaptic event begins when the hippocampus receives primary sensory inputs via the Perforant pathway [4]. Figure 1 depicts the pathway of the synapse as it travels through the Dentate Gyrus (DG), CA3, CA1, and ends at the subiculum. LTP is a reflection of synaptic plasticity and is the process by which the synapse increases in strength through repeated activation of its neurons until they synchronize to one another [7]. Therefore for the purpose of understanding memory consolidation, the connection between hippocampal regions CA3 and CA1 was investigated.

Diagnostic applications generally focus on the spectral content of Electroencephalography (EEG), the type of neural oscillations also popularly known as brain waves, which can be observed in EEG signals [5]. These waveforms are subdivided into bandwidths known as alpha, beta, theta, delta and ripple (Table 2). As a result, during SWRs, network oscillation is higher in CA1 than in CA3. The increase in firing frequencies of oscillations are crucial to how information is conveyed throughout the hippocampus. This project attempts to develop a method of estimating the number of connections that best facilitate these frequencies of oscillation. This was done by developing a hippocampal model that analyzes the frequencies represented in CA3 and CA1 as a function of number of synaptic connections in the RC and SC pathways.

2 Methods

In order to best model normal neurophysiological behavior, a computational model was created using Hodgkin-Huxley differential equations as governing equations for CA3 and CA1 spiking behavior. These equations are depicted below in section 2.2. Constants and parameters unique to CA3 and CA1 neuronal cells were pulled from literature, so as to best mimic normal physiological conditions, and are depicted in table 1 [9]. The model was built in python using the Brian Spiking Neural Simulator [3]. This model was created as a simplified version of a hippocampal model. The model uses only two systems, CA3 and CA1, and mimics other network input in the form of random

stimulation applied to both systems. Two types of synaptic connections were created; Schaffer Collaterals between CA3 and CA1 and recurrent collaterals within CA3, depicted in Figure 2.

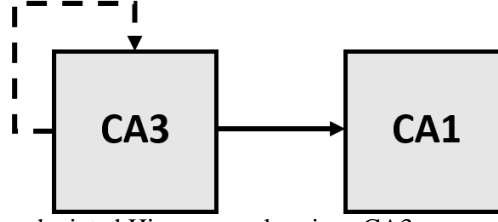


Figure 2: Block diagram depicted Hippocampal regions CA3 connected to region CA1 via SC (bold arrow) and the RC (dashed arrow) on CA3.

2.1 Assumptions

The model was created with the following assumptions also obtained from literature [9] [16].

1. CA3 pyramidal cells receive a single black box input. This means there is one synaptic input that stimulates the entirety of region CA3.
2. The single input induces an organized activation of CA3 Neurons at a specific sharp-wave event. This means that CA3 neurons spike in an organized event which induces selective inputs to CA1.
3. CA1 is induced selectively and its pyramidal cells do not spike more than once per oscillation. This is important because in reality, neurons fire sporadically and randomly which with current available computational power, would be difficult to model.
4. A model size of 36 neurons within CA3 and 44 neurons within CA1. From literature, it has been shown that in a normal adult Sprague Dawley has approximately 36,000 neurons in CA3 and 44,000 neurons within CA1 [2]. To decrease computational requirements, this number of neurons was scaled down while maintaining the same relative number of cells within each region. It is assumed that this scaled number of neurons will still mimic normal neurophysiological function.

2.2 Equations

The model utilized the following Hodgkin-Huxley equations for Pyramidal Cells [9] in both CA3 and CA1 regions and were modeled with Brian [3] through Python.

$$C \frac{dV}{dt} = g_L(E_L - V) + g_e(E_e - V) + g_i(E_i - V) - g_{Na}m^3h(E_{Na} - V) - g_{Kd}n^4(E_K - V)$$

$$\frac{dw}{dt} = \frac{1}{\tau_w} (a(V - E_L) - w) \quad \alpha_m = \frac{0.32(13 - V + V_t)}{e^{\frac{(13-V+V_t)}{4}} - 1}$$

$$\frac{dm}{dt} = \alpha_m(1 - m) - \beta_m m \quad \beta_m = \frac{0.28(V - V_t - 40)}{e^{\frac{(V-V_t-40)}{5}} - 1}$$

$$\frac{dn}{dt} = \alpha_n(1 - n) - \beta_n n \quad \alpha_n = 0.128e^{\frac{40-V-V_t}{18}}$$

$$\frac{dh}{dt} = \alpha_h(1 - h) - \beta_h h \quad \beta_h = \frac{0.4}{1 + e^{\frac{40-V-V_t}{5}}}$$

$$\frac{dg_e}{dt} = -g_e \left(\frac{1}{\tau_e} \right) \quad \alpha_n = \frac{0.032(15 - V + V_t)}{e^{\frac{(15-V+V_t)}{5}} - 1}$$

$$\frac{dg_i}{dt} = -g_i \left(\frac{1}{\tau_i} \right) \quad \beta_n = 0.5e^{\frac{10-V-V_t}{40}}$$

2.3 Parameters

103 The following table depicts the parameters obtained from Malerba et al. 2016 [6] as well as the
 104 frequency values investigated in the results.

105 Table 1: Values of Parameters
 106

Parameter	Value	Parameter	Value
C	200 pF	Delta	2 mV
g_L	10 nS	τ_w	120 ms
E_L	-58 mV	V_T	-50 mV
a	2	V_r	-46 mV
b	100 Pa	V_{thr}	0 Mv

107
 108
 109

Table 2: Frequency Values

Waveforms	Frequency Range
Delta	< 4 Hz
Theta	4 - 8 Hz
Alpha	11 - 15 Hz
Beta	16 - 31 Hz
Gamma	32 - 140 Hz
Ripple	140 - 200 Hz

110

111 2.4 Single Neuron Spiking Behavior

112 To confirm that the model accurately generates normal physiological spiking behavior, both a
 113 random probability pair and a random neuron from both CA3 and CA1 was chosen be observed as
 114 the model was run. Figure 3, shown below, demonstrates an example of the model's capability to
 115 mimic normal spiking behavior.

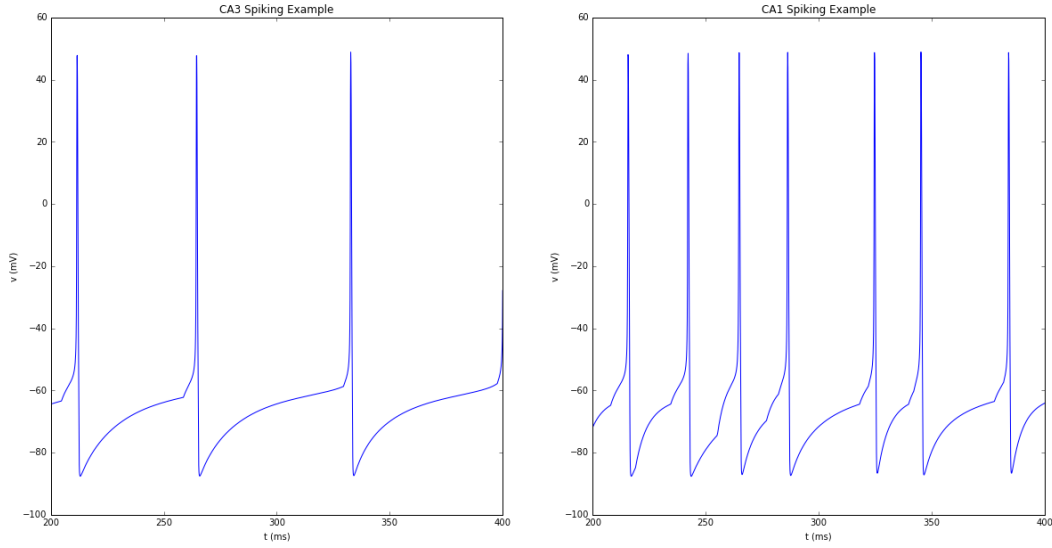


Figure 3: Spiking behavior of randomly chosen single neuron from CA3 and CA1 regions.

2.5 Synaptic Connections of Recurrent and Schaffer Collaterals

After confirming that the model worked within normal physiological parameters, the model was run one hundred times across one hundred sets of probability pairs. These probability pairs ranged from 5% to 50% probability of forming a synapse in both Recurrent and Schaffer Collaterals in increments of 5%. Spiking behavior across all neurons in both CA3 and CA1 regions were then normalized together to produce a region specific network potential. A fast Fourier transform was then applied to both network potentials to create a power spectral density measure for each frequency within physiologically relevant ranges. Figure 4, depicted below, is an example of one of the hundred probability pairs that were run.

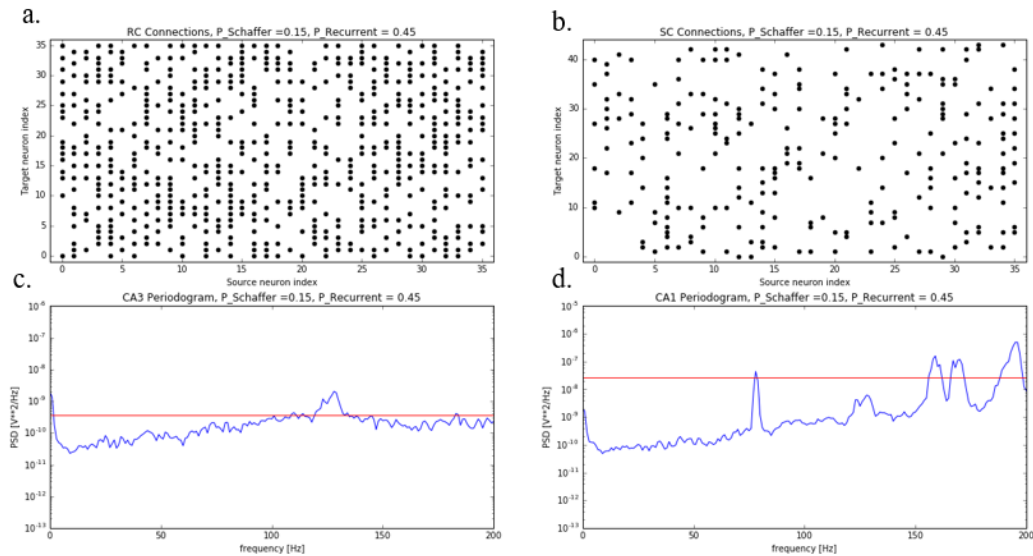
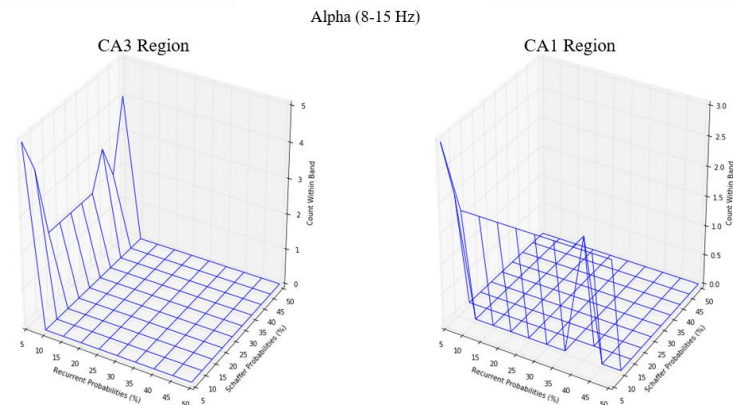


Figure 4: An excerpt of one of the 100 probability connection pairs between CA3 and CA1. a). This plot demonstrates the RC connections with SC probability $P = 0.15$ and RC $P = 0.45$. b). This plot demonstrates the SC connections with SC $P = 0.15$ and RC $P = 0.45$. c). This plot is the Power Spectral Density Plot (PSD) for CA3 pyramidal cells with given probabilities. d). This is the PSD for CA1 pyramidal cells with mentioned probabilities.

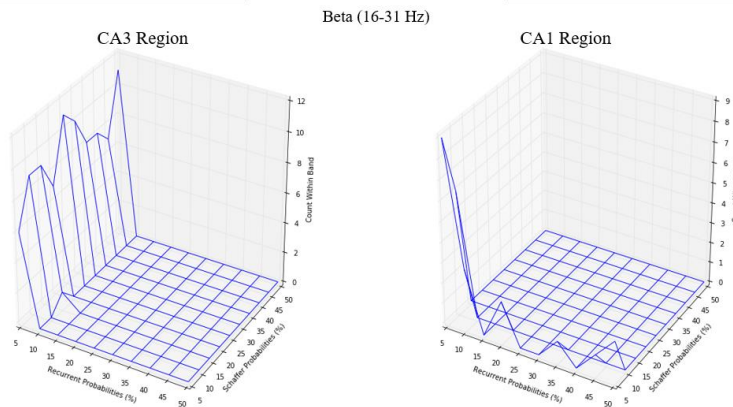
134 The frequencies most represented within each network potential was then classified and summed
 135 into its corresponding frequency band so as to best represent the relative representation of a
 136 particular frequency band with each particular probability pair. The cut off of frequencies that were
 137 chosen to represent each probability pair were those equal to at least 1.5 times that of the average
 138 power spectral density for the system and is shown as the red line pictured above in figure 4. Each
 139 probability pair along with the relative representation within each frequency band is depicted in the
 140 four 3D wire plots in the results section.

141 3 Results

142 In each of the 3D wire plots generated as a result of this project, CA3 is depicted on the left and
 143 CA1 is depicted on the right. The percentage corresponding to probability of forming synaptic
 144 connections in the Schaffer and recurrent collaterals are depicted on the X and Y coordinates of each
 145 3D wire plot with the number of relative representation within the particular band depicted on the Z
 146 coordinate.



147
 148 **Figure 5:** This figure depicts the representation of alpha oscillations in CA3 and CA1 regions.
 149 As depicted above in figure 5, the alpha frequency band is best represented within CA3 at lower
 150 recurrent probabilities and was SC connection agnostic. The opposite behavior is observed in CA1
 151 where low probabilities of SC seem to best facilitate alpha band representation while seeming to be
 152 agnostic to recurrent collateral connections.



153
 154 **Figure 6:** This depicts the frequencies in the beta range in CA3 and CA1 regions.
 155 A similar trend was observed in the CA3 region for both beta and alpha frequency bands. For CA1,
 156 however, it is shown above in figure 6 that the alpha frequency band is best facilitated with low RC
 157 and SC. This is a distinct difference between the alpha and beta frequency bands.

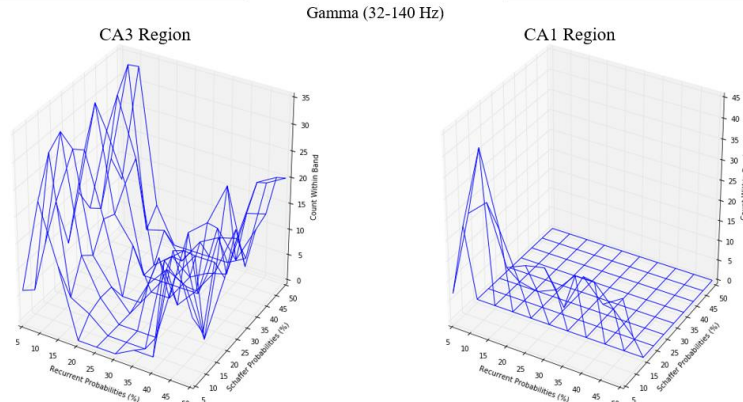


Figure 7: This figure depicts the representation of gamma oscillations in CA3 and CA1 regions.

An interesting valley is observed in figure 7 for the gamma frequency band in CA3. Very low or very high recurrent collateral probabilities facilitated neuron firing throughout all SC probabilities. A similar trend was not observed in CA1, as the plot was biased towards midline SC probabilities and low recurrent collateral probabilities.

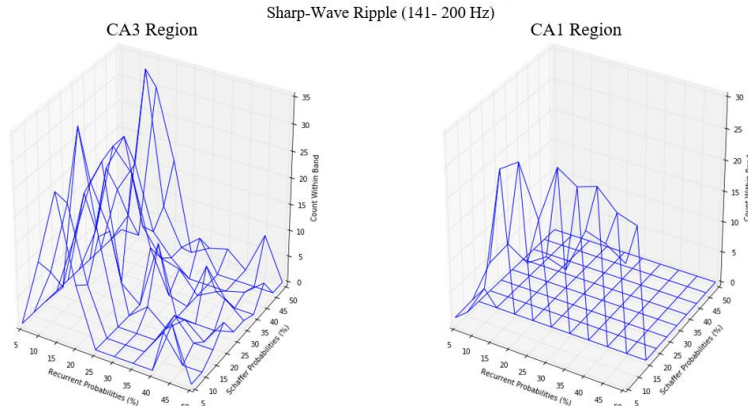


Figure 8: This depicts the frequencies in the SWR range in CA3 and CA1 regions.

Six distinct troughs were observed for ripple oscillations in CA3 region. This implied that there are distinct probabilities that can generate ripple oscillations - either low or high probabilities of both RC and SC, or low probabilities of one collateral and high probabilities of the other, or midline SC probabilities and low or high recurrent collateral probabilities. Trough-like plot was not observed in CA1 neuron firings as opposed to what was observed in CA3. For CA1, there seemed to be a bias towards midline SC probabilities and either low or high RC probabilities, unlike gamma oscillations.

4 Conclusion

As a result of analyzing the results of our model, it was determined that having approximately ten percent of CA3 neurons engaged in RC connections and ten percent of CA3 neurons engaged in SC connections, gamma and ripple frequency ranges were best facilitated and thus best mimicked normal hippocampal behavior.

While interesting, our model had many limitations that may have led to non-physiological relevant results. Namely, our model failed to produce frequencies within the delta and theta frequency ranges. This is likely due to not creating inhibitory neurons within our hippocampal model. It has been shown in literature that inhibitory neurons, although faster firing than excitatory neurons, help facilitate the lower frequency oscillations within the brain [13]. Without inhibitory neurons, our model was unable to mimic these frequency bands, regardless of the number of synaptic connections

183 chosen. Moving forward, a necessary first step when expanding this model is to differentiate
184 between excitatory and inhibitory neurons by using different set of parameters for each type.

185 Another limitation of this model is the low number of neuronal cells used. For the scope of this
186 project, and because no inhibitory neurons were modeled, the number of cells being used was kept
187 low. An assumption of this model was that this would not change the dynamics observed within the
188 system, but this would need to be verified. As such, another next step that this model should take is
189 to scale the system and see how the network behavior might change. This would need to be done
190 after first adding inhibitory neurons, however, as scaling the system without inhibitory neurons
191 would lead to overstimulation of both systems.

192 Other future steps would then be aimed at including more systems starting from the dentate gyrus,
193 followed by lateral and medial entorhinal cortex of the hippocampus. Finally, in order to extract a
194 finer local field potential, we want to model different compartments of the cell.

195 Interestingly, at gamma oscillations, there is an absence of theta rhythm in the hippocampus [15],
196 although the reason for this is yet to be determined and requires further study.

197 While limited, the model developed within this project is a step towards understanding how
198 information is conveyed within the hippocampus. Recent work has shown the importance that
199 stimulation frequencies have on conveying information. This project has been successful in showing
200 that there are non-obvious and non-linear relationships of systems within the hippocampus that these
201 frequencies are best facilitated.

202

203 **5 References**

204 [1] Axmacher, N., Mormann, F., Fernández, G., Elger, C., Fell, J. “Memory Formation by Neuronal
205 Synchronization.” *Brain Research Reviews* 52.1 (2006): 170–182. Web.

206 [2] Boss, B D et al. “On the Numbers of Neurons in Fields CA1 and CA3 of the Hippocampus of Sprague-
207 Dawley and Wistar Rats.” *Brain research* 406.1–2 (1987): 280–287. Print.

208 [3] Brette, R., Rudolph, M., Carnevale, T., Hines, M., Beeman, D., James, M., ... Destexhe, A. (2009).
209 *Strategies*, 23(3), 349–398.

210 [4] Buzsáki, G. “The Hippocampo-Neocortical Dialogue.” *Cerebral Cortex* 6 (1996): 81–92. Web.

211 [5] Buzsáki, G., Anastassiou, C. A., & Koch, C. (2012). The origin of extracellular fields and currents --
212 EEG, ECoG, LFP and spikes. *Nat Rev Neuroscience*, 13(6), 407–420.

213 [6] Fink, C. G., Gliske, S., Catoni, N., & Stacey, W. C. (2015). Network mechanisms generating abnormal
214 and normal hippocampal High Frequency Oscillations: A computational analysis. *eNeuro*, 2(3),
215 ENEURO.0024-15.2015.

216 [7] Kumar, Ashok. “Long-Term Potentiation at CA3-CA1 Hippocampal Synapses with Special Emphasis on
217 Aging, Disease, and Stress.” *Frontiers in Aging Neuroscience* 3.MAY (2011): 1–20. Web.

218 [8] Le Duigou, C., Simonnet, J., Teleńczuk, M. T., Fricker, D., & Miles, R. (2014). Recurrent synapses and
219 circuits in the CA3 region of the hippocampus: an associative network. *Frontiers in Cellular Neuroscience*,
220 7(January), 262.

221 [9] Malerba, P., Krishnan, G. P., Fellous, J. M., & Bazhenov, M. (2016). Hippocampal CA1 Ripples as
222 Inhibitory Transients. *PLoS Computational Biology*, 12(4), 1–30.

- 223 [10] Mastin, Luke. "Memory Consolidation." *Memory Processes - The Human Memory*. 2010. Web. 2 Dec.
224 2016.
- 225 [11] Morris, R., Garrud, P., Rawlins et al. "Place Navigation Impaired in Rats with Hippocampal Lesions."
226 *Nature* 1982: 681–683. Web.
- 227 [12] Rangel, Lara M. et al. "Rhythmic Coordination of Hippocampal Neurons during Associative Memory
228 Processing." *eLife* 5.JANUARY2016 (2016): 1–24. Web.
- 229 [13] Sik, A., Penttonen, M., Ylinen, A., & Buzsáki, G. (1995). Hippocampal CA1 interneurons: an in vivo
230 intracellular labeling study. *The Journal of Neuroscience: The Official Journal of the Society for*
231 *Neuroscience*, 15(10), 6651–6665.
- 232 [14] Stafstrom, Carl E., and Jong M. Rho. "Neurophysiology of Seizures and Epilepsy." Clinical Gate.
233 IKnowledge, 14 Apr. 2015. Web. 1 Dec. 2016.
- 234 [15] Sullivan, D., Csicsvari, J., Mizuseki, K., et al. . Relationships between hippocampal sharp waves, ripples
235 and fast gamma oscillation: influence of dentate and entorhinal cortical activity" .*J Neuroscience* 31.23
236 (2011): 8605–8616.
- 237 [16] Yoshida, Motoharu et al. "Stochastic Resonance in the Hippocampal CA3-CA1 Model: A Possible
238 Memory Recall Mechanism." *Neural Networks* 15.10 (2002): 1171–1183. Web.